

Structural and Optical properties of P_2O_5 -ZnO- Na_2O - Li_2O glasses

Naglaa F. Osman ^a, Mohamed M. Elokr ^b, Lalia I. Soliman ^c, Hamdia A. Zayed ^d

^a Physics Department, Modern Academy for Engineering and Technology in Maadi, Cairo, Egypt

^b Physics Department, Faculty of Science, Al-Azhar University, Cairo, Egypt

^c National Research Center, Dokki, Cairo, Egypt

^d Physics Department, Faculty of Women, Ain Shams University, Cairo, Egypt

Abstract

The transparent glasses of composition $40P_2O_5$ - $20ZnO$ -($40-x$) Na_2O - xLi_2O have been prepared using conventional melt quenching technique (where $0 \leq x \leq 25$ Li_2O mol. %). The prepared glass samples were characterized by x-ray diffraction (XRD), differential thermal analysis (DTA), UV-VIS optical absorption and Fourier transform infrared spectroscopy (FTIR). The differential thermal analysis (DTA) studies showed that the glass transition temperature (T_g) decreases from 558K to 546.7K as the content of Li_2O increases to 25 mol.% Li_2O . The density and oxygen packing density measurements are found to be increase while the molar volume decreases with increasing of Li_2O content. The FTIR studies revealed that these glasses consist of Q^3 , Q^2 , Q^1 and Q^0 structural units. Absorbance of investigated glasses was measured and used to estimate their optical absorption coefficient and optical energy gap. The optical studies revealed that the indirect optical band gap (E_g) decreases from 3.33-2.64 eV and Urbach energy increases from 0.46-2.4eV with increase of Li_2O content from zero to 25 mol.% Li_2O .

Key words: phosphate glasses, structure properties, Optical properties.

1. Introduction

The synthesis and physical properties of phosphate glasses have attracted much attention because of their potential application in technology. Phosphate glasses possess a series of interesting and unique physical properties better than other glasses such as hardness, transparency at room temperature, sufficient strength, low glass transition temperature, excellent corrosion resistance, high electrical conductivity, low melting and softening temperature and high thermal expansion [Yahia H. Elbashar et al. (2016), R. K. Brow et al (1995), Samir Y. Marzouk et al (2009), A. Bhide et al (2007), R. K. Brow (2000), I. Abrahams et al (2000)]. Among oxide glasses, sodium and lithium phosphate glasses/glass-ceramics are used as solid electrolytes for battery applications [Paramjyot Komar Jha et al (2015), A. Yamano et al (2014)]. Phosphate glasses have been considered as a promising group of glasses for optical amplifiers, fibers, etc. [A.V. Chandrasekhar et al (2003), Nehal Aboufotoh et al (2014)] and also play various important roles in laser systems.

*Corresponding Author : hamdia44@yahoo.com

For laser application glasses used as transmitting optical components, as modulators, for photonic switching and magneto-optic materials [D. D. Ramteke et al (2017)]. By varying the glass composition, glasses with specific properties can be achieved. Several studies have been shown that a chemical durability of phosphate based glasses can be improved by the addition of various oxides[S. T. Reis et al (1998), D. E. Day et al (2001)]. It is found that, the chemical durability of

phosphate glasses improved by the addition of ZnO because Zn^{2+} ion acts as an ionic cross linker between different phosphate anions, inhibiting hydration reaction. ZnO acts as a glass modifier, where Zn^{2+} occupies interstitial sites in glass network [D. Carta et al (2009)]. With the addition of ZnO to phosphate glasses, the P—O—P bonds are replaced by more chemically durable P—O—Zn bond [R. K. Brow et al (1995)]. The addition of ZnO to phosphate glasses is interesting because the ZnO – P₂O₅ systems show unusual change in correlation between the structural and optical properties (e.g.: mass density, refractive index and ultraviolet absorption edge) at the metaphosphate composition [P. M. V. Teja et al (2012)].

In literature we find that the optical property of P₂O₅ – ZnO – Na₂O – Li₂O glass system have not been studied extensively for this reason, the present work gives the preparation of 40P₂O₅-20ZnO-(40-x)Na₂O-xLi₂O glasses containing varying concentration of Li₂O reaching to 25 mol.% and the investigation of their structure and optical properties.

2. Experimental

2.1. Preparation of the glasses

The investigated glasses 40P₂O₅-20ZnO-(40-x)Na₂O-xLi₂O (0 ≤ x ≤ 25) were prepared by the conventional melt quenching technique using high purity analytical grade chemicals (NH₄)₂HPO₄, ZnO, Na₂CO₃ and LiCl as the raw material. The appropriate quantity of these chemicals were weighted and mixed in agate mortar and were hand ground for about one hour. The weighted batches were heated in an electric furnace at 673K for 1/2 h in porcelain crucibles to evaporate the ammonia then melted at 1273K for 1 h with intermediate stirring to achieve the homogeneity of the melt. So, samples of the desired shape were obtained by quenching the melt at 623K on a stainless steel mold for 2h to eliminate the mechanical and thermal stresses produced during casting left to cool to room temperature. The 40P₂O₅-20ZnO-(40-x)Na₂O-xLi₂O glasses varied from 0 to 25 mol. % in steps of 5 mol. %. The prepared glass samples were polished by silicon carbide water proof abrasive papers of various grades ranging between 320 and 1000 to achieve a good optical transparency samples.

2.2. Density measurements

The density (ρ) of the glass samples was determined at room temperature by the standard Archimedes principle using toluene as an immersion liquid ($\rho_x = 0.86455$ gm./cm³). The density was obtained from the relation,

$$\rho = [W_a / (W_a - W_b)] \cdot \rho_x, \quad (1)$$

Where, W_a is the weight of the glass sample in air, W_b is the weight of the glass sample when immersed in toluene. The relative error in these measurements was about 1 mg/cm³. Also, the molar volume (V_M) and the oxygen packing density (OPD) of the glass samples were calculated by using the molecular weight (M) and density (ρ) according to the following relations.

$$V_M = M / \rho \quad (2),$$

and
$$OPD = 1000 \cdot (\rho / M) \cdot n \quad (3)$$

Where, n is the no. of oxygen atoms per formula unit.

2.3. X- ray Diffraction measurements (XRD)

The amorphous nature of synthesized glass samples was checked by PANalytical X'Pert PRO diffractometer using CuK α target of wavelength 1.5406 Å and scanning rate 2 °/min. XRD patterns were recorded in 2 θ range between 4 ° and 80 °.

2.4. Differential Thermal Analysis (DTA)

The glass transition temperature (T_g) and the crystallization temperature (T_C), were evaluated for all the glass samples by using SDT Q600 V20.9 and scanned at a heating rate 10 ° C/min.

2.5. Infrared absorption measurements (FT-IR)

The infrared absorption spectra of the 40P₂O₅-20ZnO-(40-x)Na₂O-xLi₂O glasses were measured at room temperature in the wave number range 400-4000 cm⁻¹ by a Fourier transform computerized infrared spectrometer type, JASCO, FT/112 - 43, Japan. The prepared glasses were mixed with KBr in the ratio 2 : 200 mg glass powder : KBr, respectively. Then the weighted mixture was subjected to a pressure 5 tons/cm² to produce clear homogeneous discs. The infrared absorption measurements were measured immediately after preparing the discs.

2.6. Optical properties

The optical absorption of the glass samples were recorded at room temperature using a double beam Cary 100 spectrophotometer (model UV-12) in the wavelength range 200-900 nm. The uncertainty in the wavelength is found to be ± 1 nm.

3. Results and Discussion

3.1. Density and molar volume

The values of density (ρ) and molar volume (V_M) of all the glass samples have been calculated and their values are displayed in Table 1. Variation of density and molar volume with mol. % of Li₂O is shown in Fig.1. Density is found an increase with increasing the content of Li₂O in all glasses. This behavior of density is due to the electron negativity of Zn⁺ (1.65) is the most bigger than Na⁺ (0.93) and Li⁺ (0.98) which is responsible to compact the glass network and increases the density of glasses and also, the field strength of Li₂O (0.21) attracts the oxygen ions more than Na₂O (0.17), leading to an increase in the density [P.K. Jha et al (2015)]. The molar volume (V_M) decreases linearly with increasing the Li₂O content, this indicates a compact structure with less polymerization due to the shortened chain which confirming that the glass network became good compactable

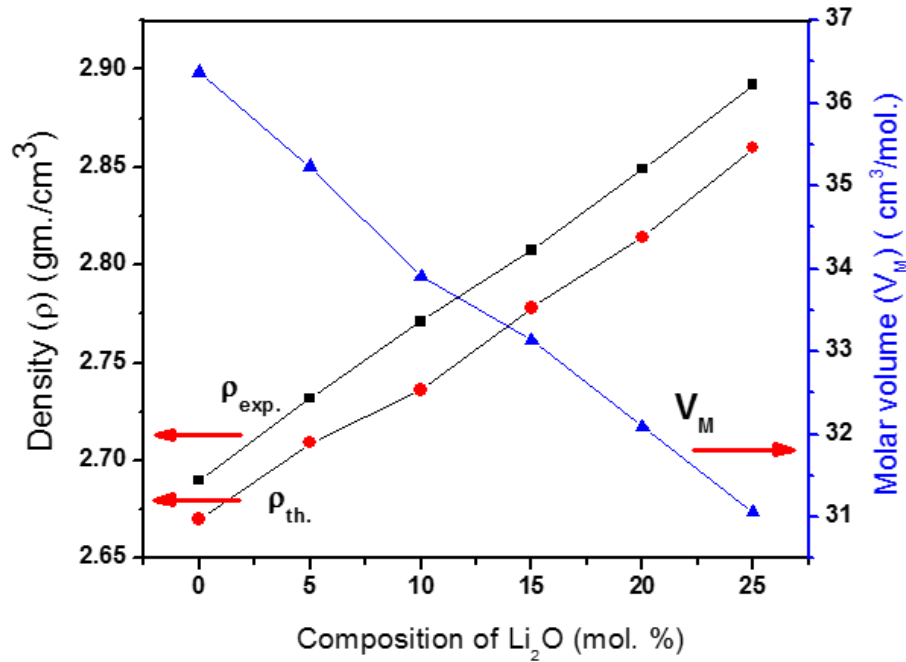


Fig.1. Variation of density (ρ) and molar volume (V_M) with composition of Li_2O mol. %.

Oxygen packing density (OPD) is a measure of the tightness of packing of the oxide network which increases linearly with increasing the Li_2O content as in Fig.2. This also indicates that the structure more packed together.

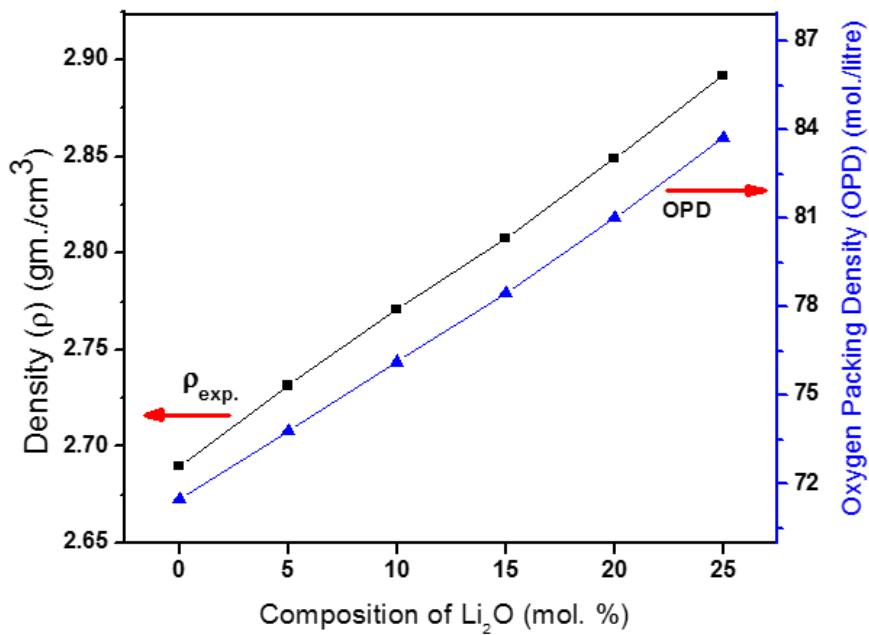


Fig.2. Variation of Oxygen packing density (OPD) with composition of Li_2O mol. %

Table 1: Density (ρ), molar volume (V_M), and oxygen packing density (OPD) of the $40P_2O_5-20ZnO-(40-x)Na_2O-xLi_2O$ glass samples.

Compositions of the $40P_2O_5-20ZnO-(40-x)Na_2O-xLi_2O$ glasses (X in mol. %)	Theoretical density $\rho_{th.}$ (gm./cm ³)	Experimental density $\rho_{exp.}$ (gm./cm ³)	Molar volume V_M (cm ³ /mol.)	Oxygen packing density OPD (mol./litre)
0	2.680	2.690	36.37	71.48
5	2.710	2.7316	35.232	73.795
10	2.736	2.7711	33.906	76.132
15	2.778	2.8077	33.134	78.468
20	2.814	2.8492	32.089	81.025
25	2.860	2.8920	31.059	83.712

3.2. X- ray Diffraction measurements (XRD)

XRD Patterns of the $40P_2O_5-20ZnO-(40-x)Na_2O-xLi_2O$ glasses are shown in Fig.3. The presence of one broad humps in the range of 2θ from 15° to 40° confirming the amorphous nature of the glass.

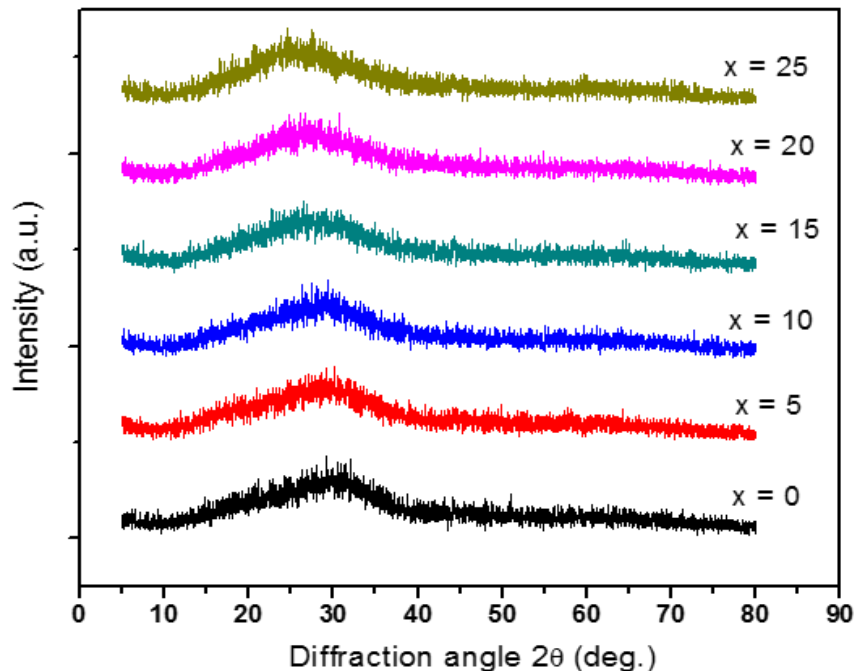


Fig.3. XRD patterns of the $40P_2O_5-20ZnO-(40-x)Na_2O-xLi_2O$ glasses with different concentrations of Li_2O mol. %

3.3. Differential Thermal Analysis (DTA)

The variation of DTA curves of the $40\text{P}_2\text{O}_5\text{-}20\text{ZnO}\text{-}(40\text{-}x)\text{Na}_2\text{O}\text{-}x\text{Li}_2\text{O}$ glasses with different concentration of Li_2O ($0 \leq x \leq 25$) are represented in Fig.4. The DTA curves are characterized by an endothermic peak corresponds to glass transition temperature (T_g) and the exothermic peak which corresponds to the crystallization temperature (T_c) [F. Wang et al (2015)].

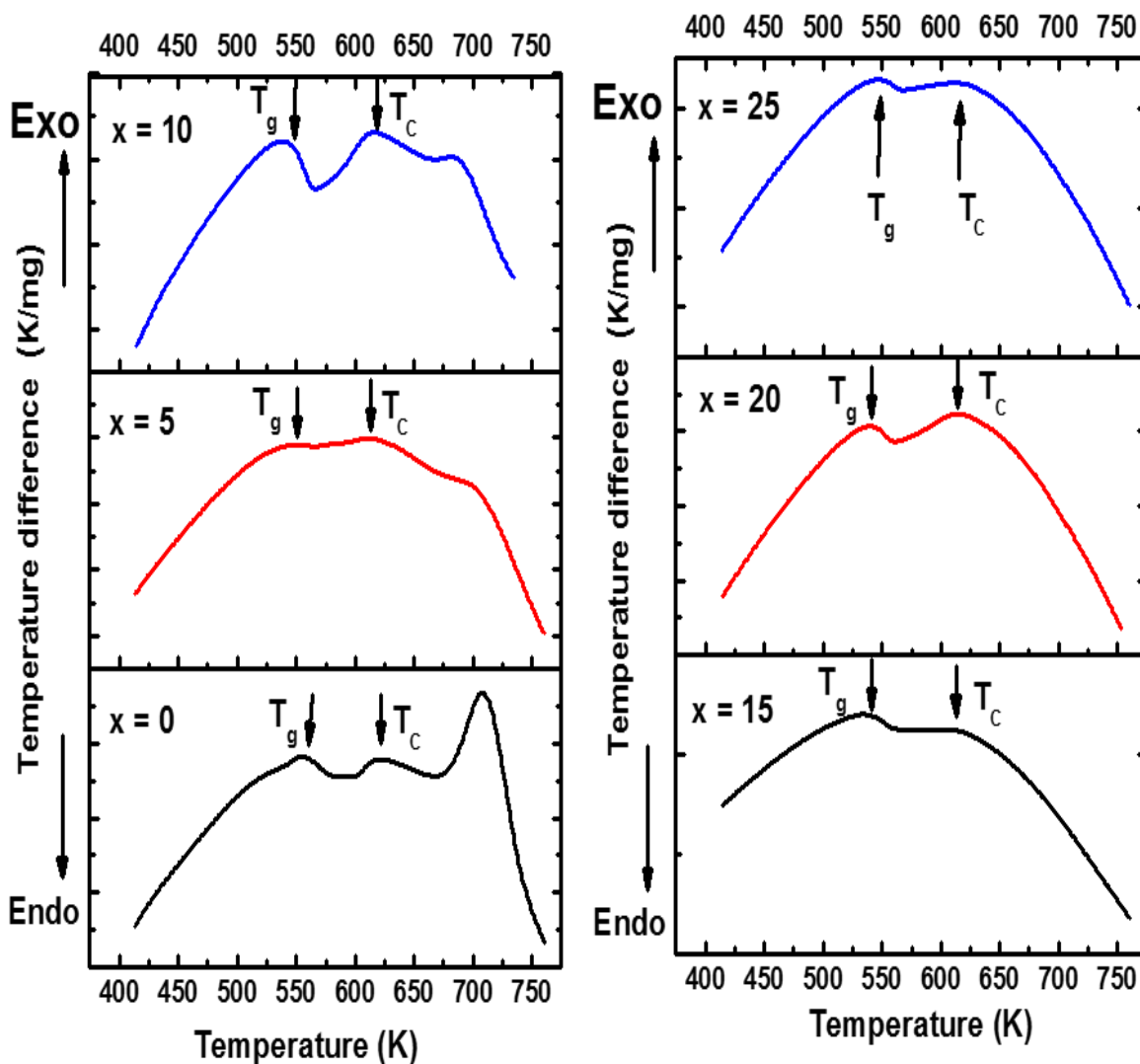


Fig. 4: DTA curves of the $40\text{P}_2\text{O}_5\text{-}20\text{ZnO}\text{-}(40\text{-}x)\text{Na}_2\text{O}\text{-}x\text{Li}_2\text{O}$ glasses with different concentrations of Li_2O mol. %

Fig. 5 shows the variation of T_g and T_c with Li_2O contents with a heating rate of 10^0 /min. It is observed from DTA measurements Table 2 that as the concentration of Li_2O increases from 0 mol. % to 25 mol.% the glass transition temperature T_g decreases because of Li_2O is a strong modifier which creates non-bridging oxygens (NBOs). The non-bridging oxygens disrupt the

long chains and break the chemical bonds [R. K. brow (2000)]. A parameter (ΔT) was obtained from $\Delta T = T_c - T_g$ which, can be used in the measurements of the glass thermal stability $H' = \Delta T / T_g$ [H. Li, X. Liang et al (2014), Y. Liu, F. Song et al (2017)]. The characteristic temperatures are calculated and presented in Table 2 & Fig.6. The value of glass thermal stability H' for the glass sample with Li_2O content 15 mol. % is found to be maximum, which indicates its highest thermal stability than other glasses.

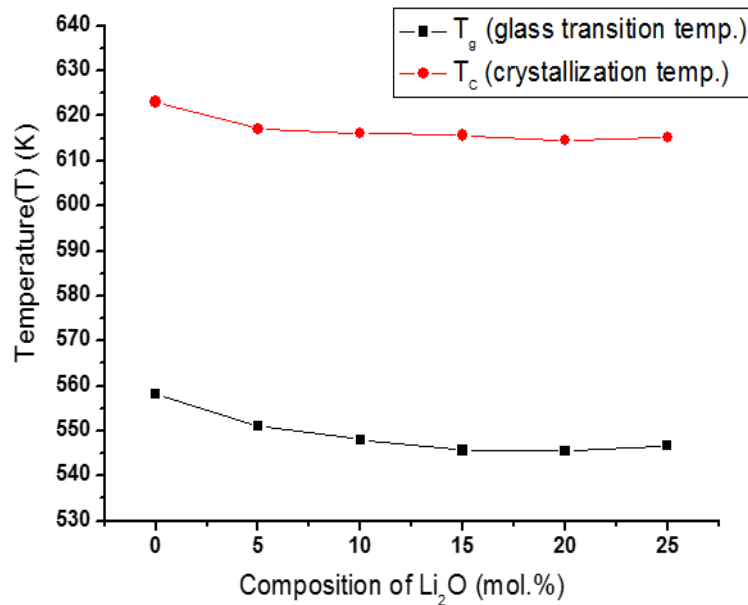


Fig. 5: Variation of Temperature (T_g & T_c) with composition of Li_2O mol. %

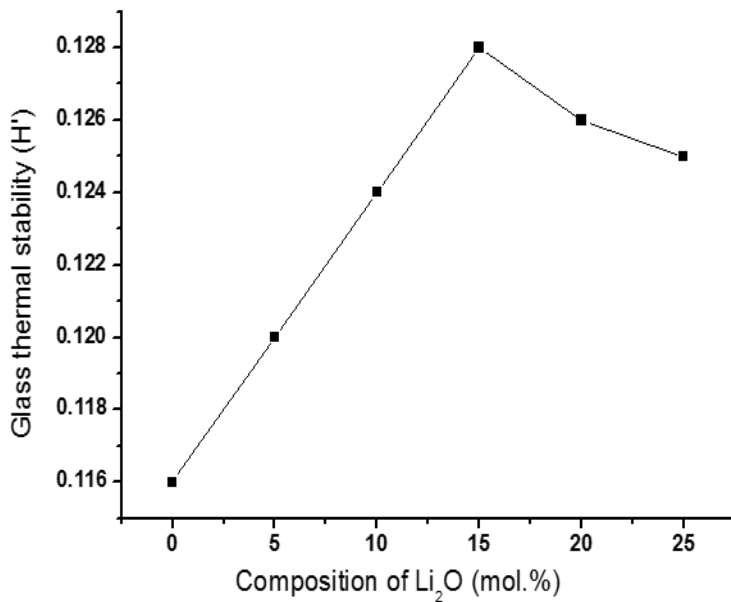


Fig. 6: Variation of glass stability (H') with composition of Li_2O mol. %

Table 2: Thermal constants observed from DTA for the 40P₂O₅-20ZnO-(40-x) Na₂O-xLi₂O glass samples.

Glass sample (X in mol. %)	Glass transition temp. T _g (K)	Crystallization temp. T _c (K)	Glass thermal stability H' = ΔT / T _g
0	558.08	623.01	0.116
5	551.15	617.1	0.120
10	548.02	616.1	0.124
15	545.6	615.6	0.128
20	545.5	614.6	0.126
25	546.7	615.2	0.125

3.4. Infrared absorption measurements (FTIR)

FTIR spectra of the 40P₂O₅-20ZnO-(40-x)Na₂O-xLi₂O glasses with different concentration of Li₂O mol.% in the frequency range of 400-4000 cm⁻¹ are shown in Fig.7 and tabulated in Table 3. The FTIR results reveal that the glasses structure network mainly consist of (O = P – O) in Q³, (P – O – P) in Q¹ and Q², PO₂ in Q² and PO₄³⁻ in Q⁰. If the modifier content increases in the phosphate matrix, phosphate structural units may be changes from Q³ → Q² → Q¹ → Q⁰ [P. K. Jha et al (2015)]. The change in structural units from Q³ to Q⁰ provides nonbridging bonds with less polymerization, which forms rigid structures due to the shortened chain length. This observation is confirmed by density and molar volume discussion of the investigated glasses. It is observed also from Fig.8 that bonds of (P – O – P) asymmetric and symmetric stretching modes shift to higher frequency as the Li₂O mol.% content increases. This shift can be explained to the increase in covalent character of (P – O – P) bonds and indicates that (P – O – P) bonds are strengthened as Li₂O substituted for Na₂O and P₂O₅.

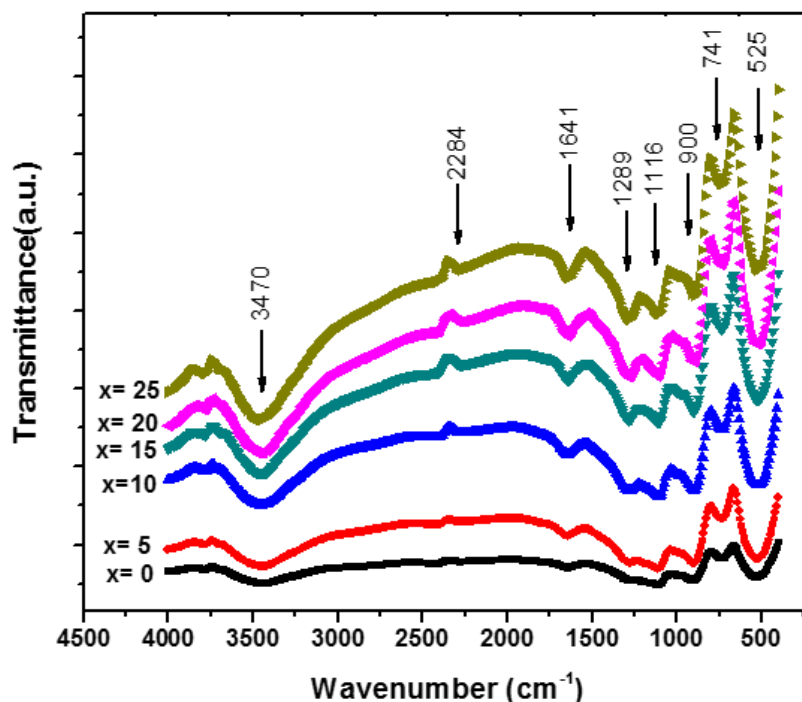


Fig. 7: FTIR spectra of the $40\text{P}_2\text{O}_5\text{-}20\text{ZnO}\text{-(}40\text{-x)Na}_2\text{O-xLi}_2\text{O}$ glasses with different concentrations of Li_2O mol. %

The shift of these bands at a higher region ($520.91 \rightarrow 533.52 \text{ cm}^{-1}$) and ($732.17 \rightarrow 765.79 \text{ cm}^{-1}$), designates the bending vibration of $\text{O}=\text{P}-\text{O}$ bonds, and $\text{P}-\text{O}-\text{P}$ symmetric stretching group in Q^1 structural units respectively [C. Dayanand et al (1996), Y. M. Lai et al (2011)]. The band between ($895.51 \rightarrow 906.09 \text{ cm}^{-1}$) corresponding to asymmetric stretching vibration of $\text{P}-\text{O}-\text{P}$ groups in Q^2 structural unit [G.V. Rao et al (2014)]. There are two weak peaks (993.12 and 1002.69 cm^{-1}) which appear in $x = 15\%$ & 20% of Li_2O content and disappear in lower & higher concentration. This band is due to PO_4^{3-} symmetric stretching groups in Q^0 structural unit [C. Dayanand et al (1996)]. Also, the band ($1108.36 \rightarrow 1125.65 \text{ cm}^{-1}$) is due to PO_4^{3-} symmetric stretching groups in Q^0 structural unit [R. L. Frost et al (2013)]. The asymmetric stretching modes of PO_2 group in Q^2 structural unit are appeared in ($1270.64 \rightarrow 1302.44 \text{ cm}^{-1}$) [Y. Tsunawaki (1981)]. It can be observed that in all glasses that these bands ($1640.99 \rightarrow 1645.18 \text{ cm}^{-1}$) and ($2263.33 \rightarrow 2280.71 \text{ cm}^{-1}$) are due to the bending vibration of H_2O molecules [F. H. Elbatal (2008), F. H. Elbatal (2011)]. A certain shift in the band ($3442 \rightarrow 3472 \text{ cm}^{-1}$) presents in all the investigated glass samples is associated with the oscillations of symmetric stretching of $\text{O}-\text{H}$ group [N. S. Hussain et al (2004)]. A certain shift in this band at higher region ($3442 \rightarrow 3472 \text{ cm}^{-1}$) designates the enhancement of OH group.

Table 3: FTIR bands of the 40P₂O₅-20ZnO-(40-x) Na₂O-xLi₂O glasses (0 ≤ x ≤ 25 mol. %)

Wave numbers (cm ⁻¹)						Assignments
X=0	X=5	X=10	X=15	X=20	X=25	
528.36	520.91	520.96	525.22	531.0	533.52	Bending vibration of (O=P—O) bond
732.17	734.68	733.68	741.92	754.66	765.79	Symmetric stretching of (P—O—P) group in Q ¹ structural unit
903.05	897.75	895.51	900.47	901.34	906.09	Asymmetric stretching of (P—O—P) group in Q ² structural unit
----	----	----	993.19	1002.69	----	Symmetric stretching of (PO ₄ ³⁻) group in Q ⁰ structural unit
1109.27	1108.36	1109.80	1116.19	1116.13	1125.65	Symmetric stretching of (PO ₄ ³⁻) group in Q ⁰ structural unit
1270.64	1280.09	1286.39	1289.60	1287.06	1302.44	Asymmetric stretching of (PO ₂) group in Q ² structural unit
1645.18	1643.06	1643.78	1641.72	1640.99	1641.50	Bending vibration H ₂ O molecule
2276.43	2280.71	2263.33	2284.15	2285.92	2280.54	Bending vibration of (H ₂ O) molecule
3442.01	3458.42	3460.69	3470.57	3466.15	3472.41	Oscillations due to symmetric stretching of O—H group

3.5. Optical properties

The optical measurements are productive tools for understanding the band structure and evaluating the band gap width and optical parameters of both ordered and disordered materials.

Fig. 8 (a, b) show the absorbance which has been measured for the 40P₂O₅-20ZnO-(40-x)Na₂O-xLi₂O glasses. The absorbance is related to the absorption coefficient (α) and the thickness of the sample (t) through the relation eqn. (4):

$$\alpha(\nu) = (1/t) \cdot \ln \left(\frac{1}{T} \right) = (1/t) \cdot \ln A \quad (4)$$

Where, T is the transmittance, t is the thickness of the glass sample, and A is the absorbance.

The absorption coefficient for the glass samples with different concentration has been calculated as shown in Fig. 9 (a, b). The relationship between the absorption coefficient and the incident photon energy (hν) is governed by the relation [J.I. Pankove (1971), J. Tauc (1974)]:

$$\alpha(\nu) = \text{const} \cdot (h\nu - E_g)^n / h\nu \quad (5)$$

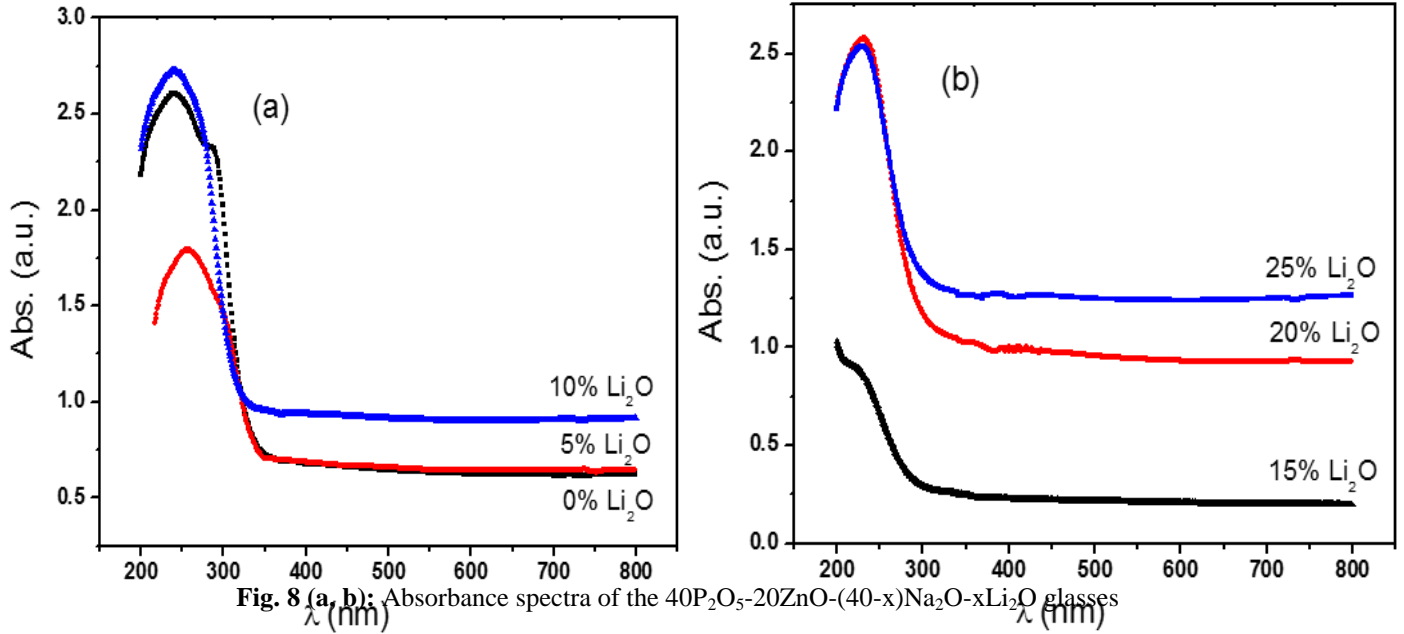


Fig. 8 (a, b); Absorbance spectra of the 40P₂O₅-20ZnO-(40-x)Na₂O-xLi₂O glasses with different concentrations of Li₂O mol. %.

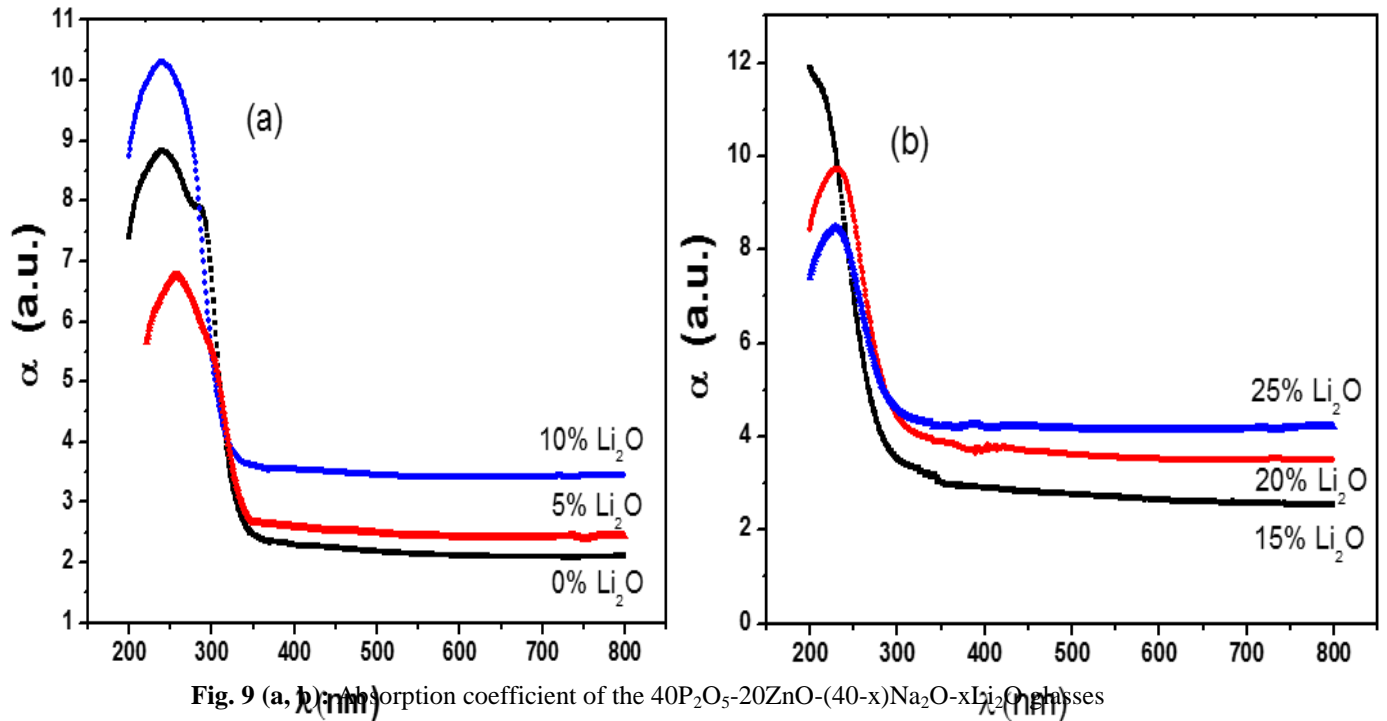


Fig. 9 (a, b); Absorption coefficient of the 40P₂O₅-20ZnO-(40-x)Na₂O-xLi₂O glasses with different concentrations of Li₂O mol. %.

where, the const. is dependent on the transition probability, E_g is the width of the band gap and n is an index that characterizes the optical absorption processes in all investigated glasses and is equal to 2, 1/2, 3, 3/2 for an indirect allowed, direct allowed, indirect forbidden, and direct forbidden transition respectively [A.F. Qasrawi (2005)]. For the amorphous material is usually corresponding to the indirect transition hence $(\alpha h\nu)^{1/2}$ was plotted against $h\nu$ as shown in Fig. 10 (a, b) for the 40P₂O₅-20ZnO-(40-x) Na₂O-xLi₂O glasses. So, the optical band gap energy was

calculated for such glasses by linear fitting of the high absorption regions. The intersection on $h\nu$ - axis corresponded to the optical band gap E_g with $(\alpha h\nu)^{1/2}$ equals zero. The relation between $\ln(\alpha)$ and $h\nu$ gives the Urbach energy which is the width of the tail of the localized states in the band gap according to the relation:

$$\alpha = \text{const} \cdot \exp. (h\nu / E_u) \quad (6)$$

$$\ln(\alpha) = (h\nu / E_u) - \text{const} \quad (7)$$

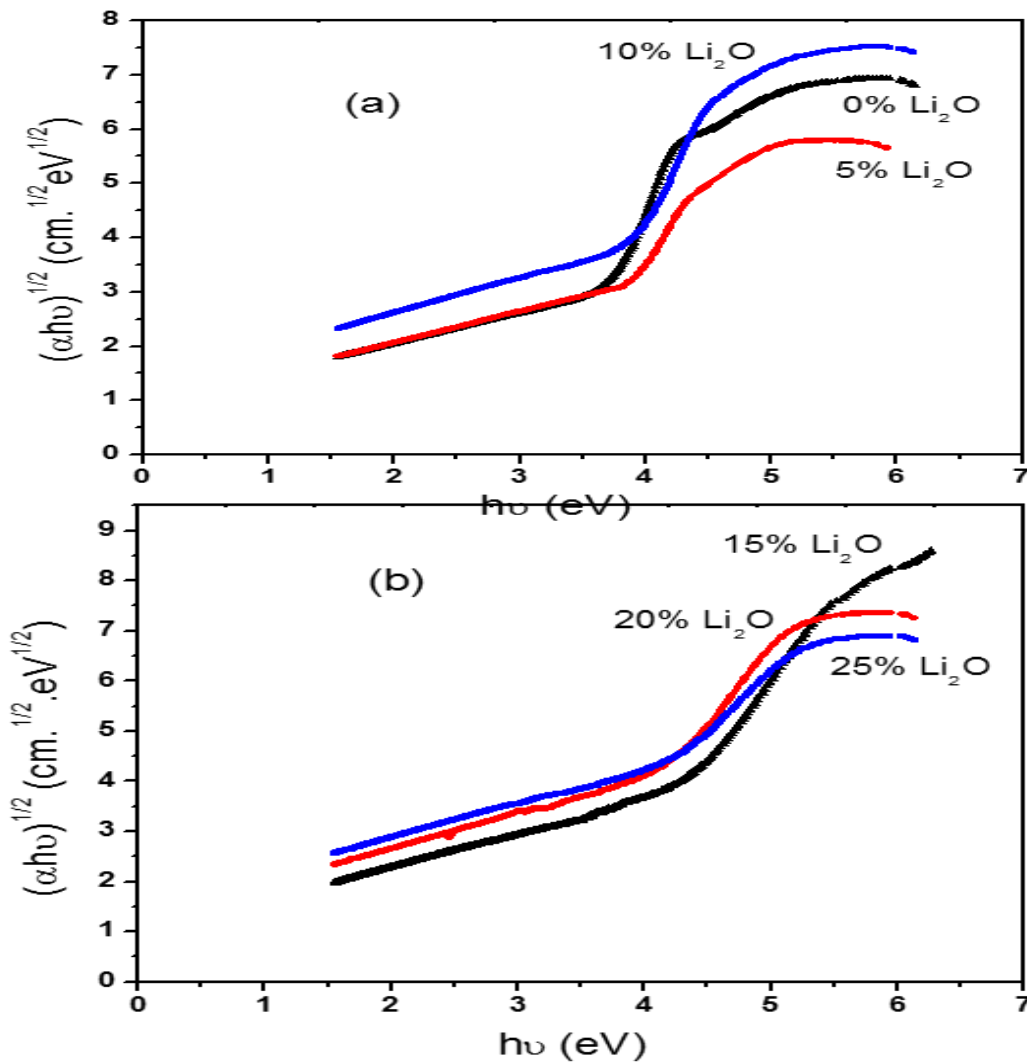


Fig. 10 (a, b): variation of $(\alpha h\nu)^{1/2}$ versus $h\nu$ for the $40\text{P}_2\text{O}_5\text{-}20\text{ZnO}\text{-}(40\text{-x})\text{Na}_2\text{O}\text{-xLi}_2\text{O}$ glasses with different concentrations of Li_2O mol. %.

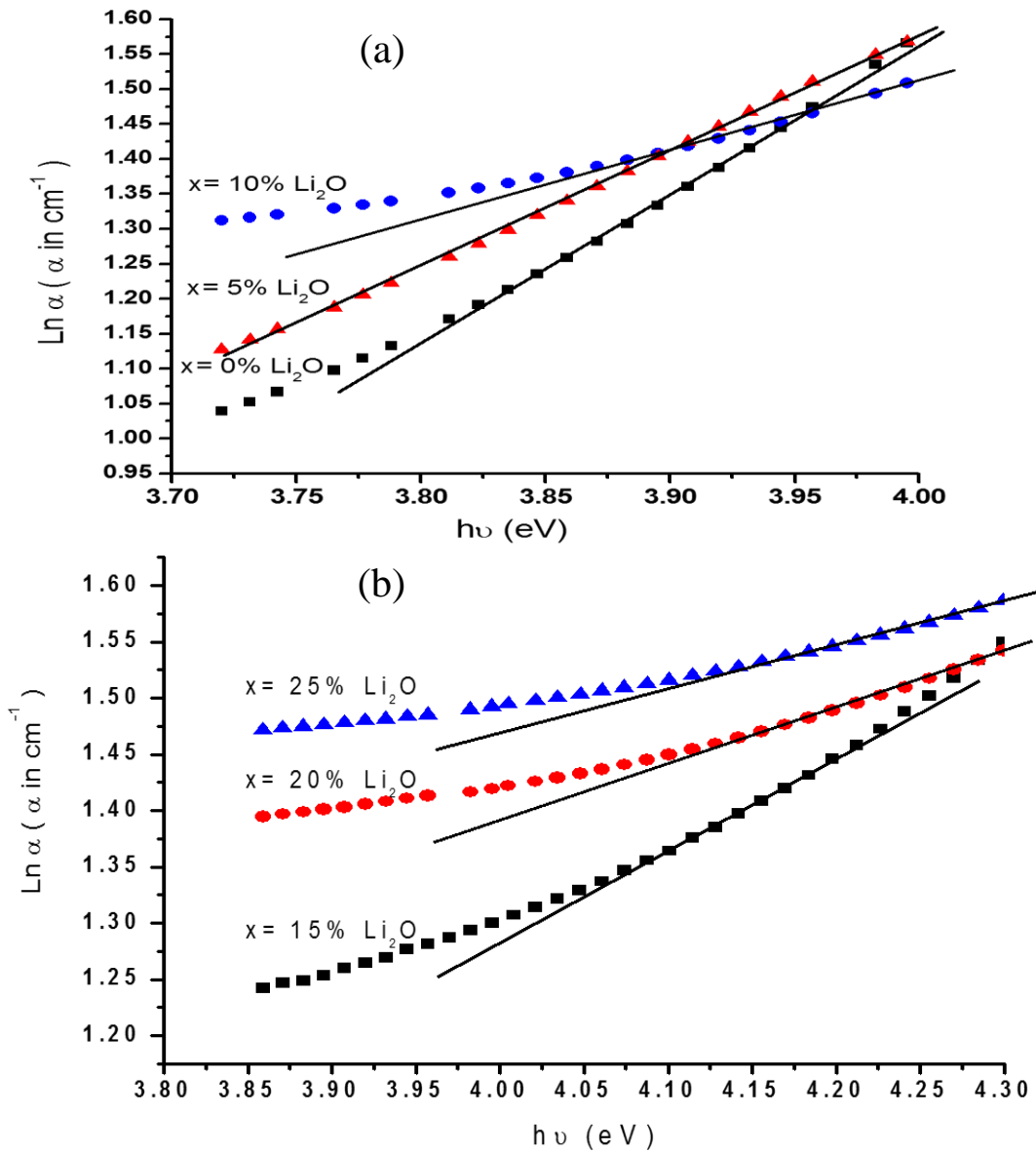


Fig. 11 (a, b): $\text{Ln } \alpha$ versus $h\nu$ for the $40\text{P}_2\text{O}_5\text{-}20\text{ZnO}\text{-}(40\text{-}x)\text{Na}_2\text{O}\text{-}x\text{Li}_2\text{O}$ glasses with different concentrations of Li_2O mol. %.

In the present study, Urbach energy can be presented as in Fig. 11 (a, b) for samples contain Li_2O ($x = 0, 5, 10, 15, 20, 25$ mol. %). It is found that the energy gap E_g decreases from 3.33 to 2.64 eV by increasing Li_2O content and Urbach energy increases from 0.46 to 2.4 eV which are represented in Fig.12.

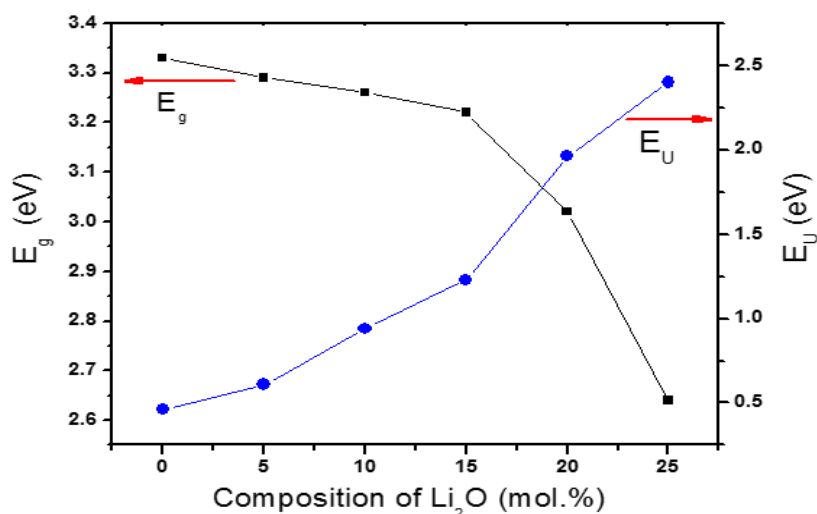


Fig. 12: Optical energy gap & Urbach energy for the 40P₂O₅-20ZnO-(40-x)Na₂O-xLi₂O glasses with different concentrations of Li₂O (mol. %).

4. Conclusion

The structural and optical properties of the 40P₂O₅-20ZnO-(40-x)Na₂O-xLi₂O glasses ($0 \leq x \leq 25$ mol. % Li₂O) prepared by conventional melt quenching technique were investigated. The results show that all prepared glasses are amorphous in nature. The replacement of Na₂O by Li₂O decreases the glass transition temperature (T_g). The glass sample with Li₂O content 15 mol. % exhibits highest thermal stability. It is found that the experimental density ρ_{exp} and theoretical density ρ_{th} increase with increasing Li₂O mol. %, while the molar volume exhibits opposite trend to that of density. The FTIR results reveal that the glasses structure network mainly consists of Q³, Q², Q¹ and Q⁰ structural units. The phosphate structural units may be changes from Q³ to Q⁰ by increasing the modifier content and provides nonbridging bonds with less polymerization.

References

- A. Bhide, K. Hariharan**, Mater. Chem. Phys.105 (2007) 213.
- A.F. Qasrawi**, Cryst. Res. Technol., 40 (2005) 610-614.
- A. V. Chandrasekhar, A. Radhapaty, B. I. Reddy**, Opt. Mater. 22 (2003) 215.
- A. Yamano, M. Morishita, G. Park, T. Sakamoro, H. Yamauchi, T. Nagakane, M. Ohji, A. Sakamoto, T. Sakai**, J. Electrochem. Soc. 161 (2014) A1094-A1099.
- C. Dayanand, G. Bhikshamaiah, V. Jaya Tyagaraju, M. Salagram, A.S.R. Krishna Murthy, J. Mater. Sci. Lett.** 31 (1996) 1945.
- D. Carta, J. Knowles, P. Guerry, M. Smith, R. New. Port**, J. Mater. Chem., 19 (2009) 150-158.
- D. E. Day, Z. Wu, C. S. Ray and P. Hrna**, J. Non-Cryst. Solids, 241, 1 (1998).
- D. D. Ramteke, R. E. Kroon, H. C. Swart**, J. Non-Cryst. Solids 457 (2017) 157-163.
- F. H. Elbatal**, J. Mater. Sci. 43 (2008) 1070-1079.
- F. H. Elbatal, M. A. Marzouk, A. M. Abdelghany**, J. Non-Cryst. Solids 357 (2011) 1027-1036.
- F. Wang, Q. Liao, Y. Dai, H. Zhu**, Mater. Chem. Phys, 166 (2015) 215-222.
- G.V. Rao, H. D. Shashikala**, J. Adv. Ceram. 3 (2014) 109-116.
- H. Li. X. Liang, C. Wang, H. Yu. Z. Li. S. Yang**, J. Mol. Struct. 1076 (2014) 592-599.
- I. Abrahams, E. Hadzifejzovic**, Solid State Ionic 134 (2000) 249.
- J. Tauc, Amorphous and Liquid Semiconductors**, New York: Plenum Ch. 4, 1974.
- J.I. Pankove**, Optical Processes in Semiconductors, New Jersey, Prentice-Hall, 1971.
- N. S. Hussain, M.A. Lopes, J. D. Santos**, Mater. Chem. Phys. 88 (2004) 5.
- Nehal Aboufotouh, Yahia El bashar, Mohamed Ibrahim, Mohamed El Okr**, Ceramics International 40 (2014) 10305-10399.
- P. K. Jha, O. P. Pandey, K. Singh**, J. Mol. Struct. 1094 (2015) 174-182.
- P. M. V. Teja, C. Rajyasree, P. S. Rao, A. R. Babu, C. Tirupataiah, D. K. Rao**, J. Mol. Struct. 1014 (2012) 119-125.
- P.K. Jha et al**, Journal of Molecular Structure 1094 (2015) 174 -182.
- Paramjyot Komar Jha, O. P. Pandey, K. Singh**, J. Mol. Struct. 1094 (2015) 174-182.

R. K. Brow, D. R. Tallant, S. T. Myers and C. C. Phifer, J. Non- Cryst. Solids, 191, 45, (1995).

R. L. Frost, Y. Xi. R. Scholz, F. M. Belotti, M. C. Filho, Spect. Lett. 46 (2013) 415-420.

R. K. Brow, J. Non-Cryst. Solids, 1 (2000) 263-264.

S. T. Reis, M. Karabulut and D. E. Day, J. Non-Cryst. Solids, 292, 150 (2001).

Samir Y. Marzouk, Materials Chemistry and Physics 114 (2009) 188-193.

Y. Liu, F. Song, G. Jia, Y. Zhang, Y. Tang, Results in Physics 7 (2017) 1987-1992.

Y. M. Lai, X. F. Liang, S. Y. Yang, J. X. Wang, L. H. Cao, B. Dai, J. Mol. Struct. 992 (2011) 84-88.

Y. Tsunawaki, J. Non-Cryst. 44 (1981) 369-378.

Yahia H. Elbashar, Ali M. Badr, Haron A. Elshaikh, Ahmed G. Mostafa, Ali M. Ibrahim,
Processing and Application of Ceramics 10 (4) (2016) 277-286.

المخلص باللغة العربية

الخواص التركيبية و الضوئية لزجاج أكسيد فوسفات الزنك الصوديوم الليثيوم

^a نجلاء فتحي عثمان، ^b محمد محمود العقر، ^c ليلي ابراهيم سليمان، ^d حمدي عبد الحميد زايد

^a مدرس مساعد - قسم الفيزياء - الأكاديمية الحديثة للهندسة و التكنولوجيا - القاهرة - مصر

^b استاذ فيزياء الجوامد - قسم الفيزياء - كلية العلوم - جامعة الأزهر - القاهرة - مصر

^c استاذ فيزياء الجوامد - قسم الفيزياء - المركز القومي للبحوث - القاهرة - مصر

^d استاذ فيزياء الجوامد - قسم الفيزياء - كلية البنات - جامعة عين شمس - القاهرة - مصر

في هذا البحث تم تحضير زجاج شفاف من $40 \text{ P}_2\text{O}_5 - 20 \text{ ZnO} - (40-x) \text{ Na}_2\text{O} - x \text{ Li}_2\text{O}$ حيث ان $(0 \text{ mol. \%} \leq X \leq 25 \text{ mol. \%})$ باستخدام تقنية حيود أشعة اكس (XRD) و التحليل الحرارى التفاضلى (DTA) و الامتصاص الضوئى للأشعة المرئية و فوق بنفسجية (UV-VIS optical absorption) و قياسات تحول فورييه للأشعة تحت الحمراء (FTIR). اظهرت دراسات التحليل الحرارى التفاضلى (DTA) أن درجة التحول للزجاج (T_g) تقل من 558 K الى 546.7 K مع زيادة تركيز Li_2O الى 25 mol. %. وكذلك وجد أن قياسات الكثافة (ρ) و كثافة الحزمة الأوكسجينية (OPD) تزيد بينما الحجم المولارى (V_m) يقل مع زيادة تركيز Li_2O . أثبتت دراسات (FTIR) ان هذه الزجاجيات تتكون من Q^0, Q^1, Q^2, Q^3 وحدة تركيبية. و قد تم قياس الامتصاص لهذه الزجاجيات و التى استخدمت لحساب معامل الامتصاص الضوئى و طاقة الفراغ الضوئى. و اثبتت الدراسات الضوئية أن طاقة الفراغ الضوئى الغير مباشر (E_g) تقل من 3.33 eV الى 2.46 eV و أن طاقة أوربخ تزيد من 0.46 eV الى 2.4 eV مع زيادة تركيز Li_2O من الصفر الى 25 mol. %.